CLINICAL AND VACCINE IMMUNOLOGY, Nov. 2010, p. 1781–1789 Vol. 17, No. 11
1556-6811/10/$12.00 doi:10.1128/CVI.00277-10

A Single, Engineered Protein Therapeutic Agent Neutralizes Exotoxins from Both *Staphylococcus aureus* and *Streptococcus pyogenes*▽†

Ningyan Wang,[1] Daiva M. Mattis,[1] Eric J. Sundberg,[2] Patrick M. Schlievert,[3] and David M. Kranz[1]*

Department of Biochemistry, University of Illinois, Urbana, Illinois 61801[1]; Boston Biomedical Research Institute, Watertown, Massachusetts 02472[2]; and Department of Microbiology, University of Minnesota Medical School, Minneapolis, Minnesota 55455[3]

Received 7 July 2010/Returned for modification 25 August 2010/Accepted 13 September 2010

***Staphylococcus aureus* and *Streptococcus pyogenes* secrete exotoxins that act as superantigens, proteins that cause hyperimmune reactions by binding the variable domain of the T-cell receptor beta chain (Vβ), leading to stimulation of a large fraction of the T-cell repertoire. To develop potential neutralizing agents, we engineered Vβ mutants with high affinity for the superantigens staphylococcal enterotoxin B (SEB), SEC3, and streptococcal pyrogenic exotoxin A (SpeA). Unexpectedly, the high-affinity Vβ mutants generated against SEB cross-reacted with SpeA to a greater extent than they did with SEC3, despite greater sequence similarity between SEB and SEC3. Likewise, the Vβ mutants generated against SpeA cross-reacted with SEB to a greater extent than with SEC3. The structural basis of the high affinity and cross-reactivity was examined by single-site mutational analyses. The cross-reactivity seems to involve only one or two toxin residues. Soluble forms of the cross-reactive Vβ regions neutralized both SEB and SpeA *in vivo*, suggesting structure-based strategies for generating high-affinity neutralizing agents that can cross-react with multiple exotoxins.**

Toxic shock syndrome (TSS) was characterized as an illness associated with *Staphylococcus aureus* infection 30 years ago (15, 43, 50). Shortly thereafter, toxic shock syndrome toxin 1 (TSST-1) from *S. aureus* was identified as the protein primarily responsible for the illness, including all cases of menstrual TSS and one-half of nonmenstrual cases (4, 41). More recently, staphylococcal enterotoxins, notably serotypes B (SEB) and C (SEC), have been associated with the other one-half of nonmenstrual cases. In the late 1980s, streptococcal pyogenic exotoxins (Spes), produced by *Streptococcus pyogenes*, were associated with causation of streptococcal TSS (14, 46). TSST-1, along with SEs and Spes, is a member of a large family of molecules secreted by *S. aureus* and *S. pyogenes* that cause fever and hypotension and that have systemic effects leading to circulatory and respiratory distress and organ failure (27, 32, 34). More recent studies have implicated these toxins as virulence factors and as contributing factors to other human diseases, including various cardiac diseases (1, 28, 35), severe atopic dermatitis (42), and airway diseases (3, 7, 39).

The term "superantigen" (SAg) was given to this class of molecules because the toxins were shown to stimulate a large fraction of T cells that bear the same variable regions of the T-cell receptor (TCR) beta chain (Vβ regions) (32). As up to 20% of the T-cell repertoire can bear the same Vβ region, SAgs are capable of stimulating thousands of times more T cells than conventional antigens. This massive stimulation of T cells contributes to the release of many inflammatory molecules, including tumor necrosis factor alpha (TNF-α) and interleukin-1 (IL-1), leading to a cytokine storm and the symptoms of TSS.

Soluble ligands for the TCR, such as a superantigen, cannot stimulate T cells through monovalent binding. Accordingly, SAgs act by cell-to-cell cross-linking TCRs upon simultaneous binding to the class II major histocompatibility complex (MHC) product on an antigen-presenting cell (2, 8, 29). Hence, multivalent cross-linking of TCRs and MHC class II molecules leads directly to the release of inflammatory molecules by both T cells and antigen-presenting cells. The bacterial SAg family now numbers over 50 members and includes the *S. aureus* TSST-1, SEs, and SE-like proteins A to E and G to U. *Streptococcus pyogenes* exotoxins include SpeA and -C and SpeG to -M, the mitogenic exotoxins called $SMEZ_n$, and streptococcal superantigen (34).

The three-dimensional structures of SAgs from *S. aureus* and *S. pyogenes*, all of which are 22- to 30-kDa proteins consisting of two domains, are largely similar (34). The Vβ region docks in a cleft between the two domains, although the atomic details of the contacts differ among SAg-Vβ interactions (47). Although different SAgs can bind to distinct Vβ regions, those subfamily members within a structurally related group (among five currently known groups) tend to bind to the same Vβ region(s) (34). For example, the SAgs in group II, which include SEB, SEC3, and SpeA, all bind to the mouse Vβ8 region (34). SEC3 and SpeA share 65% and 53% primary sequence identity, respectively, with SEB (34). The crystal structures of all three toxins, alone and in complex with Vβ8.2, have been solved, providing a useful structural framework (19, 30, 48).

To develop potential neutralizing agents, we previously engineered Vβ8 mutants that had up to a 2-million-fold increase in affinity for either SEB or SEC3, using a yeast (*Saccharomyces cerevisiae*) display system (9, 24). The general principle of the strategy was based on the premise that soluble forms of these Vβ proteins would bind to the same epitope on the SAg that was used in binding to the TCR. Thus, the binding of the

* Corresponding author. Mailing address: Department of Biochemistry, University of Illinois, 600 S. Mathews Ave., Urbana, IL 61801. Phone: (217) 244-2821. Fax: (217) 244-5858. E-mail: d-kranz@uiuc.edu.

† Supplemental material for this article may be found at http://cvi.asm.org/.

▽ Published ahead of print on 22 September 2010.

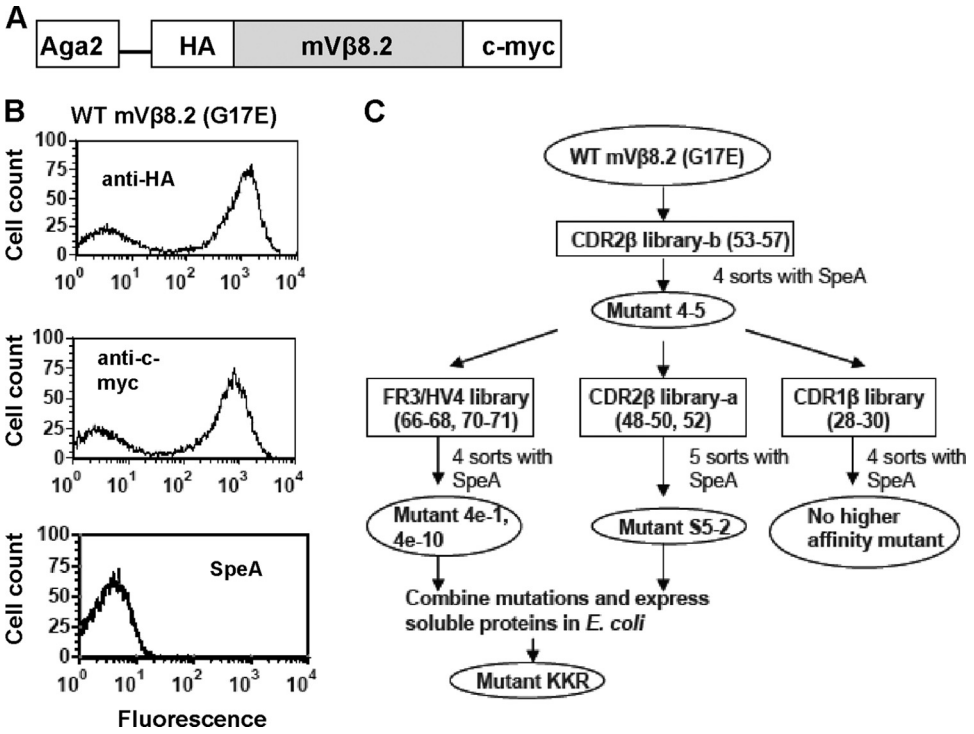

FIG. 1. Yeast display strategy to engineer high-affinity Vβ variants against SpeA. (A) Diagram of the mVβ8.2 construct; (B) flow cytometric analysis of yeast cells displaying stabilized wild-type (WT) mVβ8.2 with the stabilizing mutation G17E, stained with anti-HA antibody, anti-c-myc antibody, and 0.2 μM biotin-labeled SpeA; (C) schematic of the screening process for engineering high-affinity Vβ variants against SpeA. Four libraries (in rectangles) were constructed in the mVβ8.2 regions of CDR2, CDR1, and FR3/HV4, with the degenerate residue numbers in each library shown in parentheses. Selected high-affinity clones isolated from a library or synthesized by combination of mutations (KKR) are shown in the circles.

soluble Vβ would operate as a competitive inhibitor of the cellular reaction. Furthermore, if a sufficiently long dissociation rate could be achieved for the soluble Vβ-SAg interaction, the complexes might be cleared *in vivo* before the free SAg acted on its target cells. Toward this goal, a soluble Vβ (called G5-8) against SEB with a picomolar equilibrium dissociation constant (K_D) value was shown to be completely protective in rabbit models of TSS caused by SEB (9). Another Vβ mutant called L2CM was also engineered previously for high-affinity (low nanomolar) binding to SEC3 (24).

To begin to generate soluble Vβ regions as neutralizing agents against the *S. pyogenes* SAgs, here we engineered high-affinity Vβ8 mutants against SpeA (25). In addition, we explored the ability of this family of high-affinity proteins to cross-react with the structurally related SAgs in the group SpeA, SEB, and SEC3 (48). Unexpectedly, high-affinity Vβ regions generated against SpeA cross-reacted with SEB to a greater extent than they did with SEC3, and those Vβ regions generated against SEB cross-reacted with SpeA to a greater extent than they did with SEC3. These cross-reactivities would not have been predicted from the primary sequence similarities among the three toxins or their species of origin. The structural basis of this cross-reactivity seems to be controlled by one or two toxin residues. This cross-reactivity resulted in some Vβ variants engineered originally to bind with increased *in vitro* affinity to SEB that are capable of neutralizing SpeA *in vivo*. These results suggest a structure-based strategy for generating a single protein therapeutic agent exhibiting protective capacity toward multiple exotoxins.

MATERIALS AND METHODS

Construction and screening of Vβ8 yeast display libraries. The mouse Vβ8.2 gene was subcloned into the yeast display vector (pCT302) with an N-terminal hemagglutinin (HA) tag and a C-terminal c-myc tag (Fig. 1A). Various Vβ8 libraries with multiple randomized residues were generated by PCR using overlapping degenerate primers (with NNS codons) (9). Libraries were constructed in complementarity-determining region 2 (CDR2; residues 48 to 52 and 53 to 57), framework 3 (FR 3)/hypervariable 4(HV4; residues 66 to 68 and 70 to 71), and CDR1 (residues 28, 29, and 30) using the Vβ8.2 gene (with mutation G17E) or first-generation mutants as templates. Yeast cells were stained with biotin-labeled SpeA (Toxin Technology, Sarasota, FL) at concentrations varying from 1 μM to 0.1 nM, followed by incubation with streptavidin-phycoerythrin (PE) (1:2,000 dilution; BD Biosciences). Cells were examined by flow cytometric sorting (MoFlo; Cytomation), and the top 1% of fluorescent cells were collected and cultured for subsequent sorting or plating and subsequent analysis of colonies. Binding of SpeA by clones was quantitatively analyzed by flow cytometry (Accuri C6).

Mutational analysis of Vβ binding. Six mutated residues (Y47, R53, H54, V55, L56, and E57) of first-generation clone 4-5 from the CDR2 library were individually reverted to the wild-type (WT) Vβ8.2 residues (H47, G53, S54, T55, E56, and K57) by site-directed mutagenesis using a Quikchange kit (Stratagene, La Jolla, CA). Yeast cells displaying the single-site mutants were titrated with biotin-labeled SpeA at concentrations varying from 1 μM to 0.1 nM and analyzed by flow cytometry. The concentration of SpeA that yielded 50% maximal binding (BD_{50}) was calculated as an estimate of affinity (24).

Purification and binding analysis of the soluble Vβ proteins. Soluble Vβ proteins were expressed as inclusion bodies in *Escherichia coli* BL21(DE3) using the pET28 expression vector (Novagen). Proteins were refolded *in vitro* and

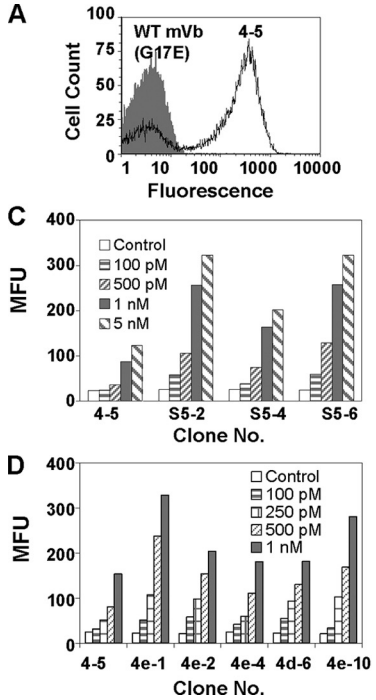

B

Clone no.	17	24	28	29	30a	30	41	42	47	48	49	50	51	52	53	54	55	56	57	66	67	68	69	70	71	72	80	81
			CDR1β						CDR2β											FR3 / HV4β								
WT	G	N	N	H	-	N	H	G	H	Y	S	Y	G	A	G	S	T	E	K	K	A	S	R	P	S	Q	E	L
WT (G17E)	E																											
4-5 (CDR2b)	E								Y						R	H	V	L	E									
S7 (CDR2b)	E														K	H	V	M	D									
S9 (CDR2b)	E														K	H	V	L	A									
S29 (CDR2b)	E														K	H	V	L										
S2-1 (CDR2a)	E								Y	S		L		V	R	H	V	L	E									
S2-2 (CDR2a)	E								Y	S		E		V	R	H	V	L	E									
S2-3 (CDR2a)	E								Y	K		F		I	R	H	V	L	E									
S2-4 (CDR2a)	E								Y			E		P	R	H	V	L	E									
S2-6 (CDR2a)	E								Y	S		G		P	R	H	V	L	E									
S5-2 (CDR2a)	E								Y	K		E		I	R	H	V	L	E									
S5-4 (CDR2a)	E								Y			L		T	R	H	V	L	E									
S5-6 (CDR2a)	E								Y			E		I	R	H	V	L	E									
4d-5 (HV4)	E								Y						R	H	V	L	E			V		S				
4e-2 (HV4)	E								Y						R	H	V	L	E	R		R		D				
4e-4 (HV4)	E								Y						R	H	V	L	E	R		V						
4e-7 (HV4)	E								Y						R	H	V	L	E	T		R		D				
4e-12 (HV4)	E								Y						R	H	V	L	E	R		R		A				
4e-10 (HV4)	E								Y						R	H	V	L	E							R		
4e-1 (CDR1)	E					K		Q	Y						R	H	V	L	E									
S2-3 (CDR1)	E			H	W	R			Y						R		V											
S3-10 (CDR1)	E			H	L	P			Y						R		V											
KKR	E					K			Y	K		E		I	K	H	V	L	E							R		
L2CM	E													V		N				E						H	V	S
G5-8	E	K		S	Y	F		E	F	M		H		I	R	N	V											
G5-8 (R53G)	E	K		S	Y	F		E	F	M		H		I	G	N	V											

FIG. 2. Characterization of SpeA-binding, high-affinity Vβ mutants isolated from yeast display libraries. (A) Flow cytometry histograms of SpeA binding to first-generation mutant 4-5 (line) and to WT mVβ8.2(G17E) (gray). Yeast cells were incubated with 20 nM (4-5) or 0.2 μM [WT mVβ8.2(G17E)] biotin-labeled SpeA. (B) Sequences of the Vβ clones isolated from the four degenerate libraries in the affinity maturation process. Only those mutants with unique sequences are shown. In parentheses are the libraries from which the mutant clones were isolated. (C and D) Selected Vβ clones isolated from the CDR2-a library (C) and HV4 library (D) were titrated with biotin-labeled SpeA (at concentrations ranging from 100 pM to 5 nM) and analyzed by flow cytometry. Mean fluorescence units (MFU) for the histograms (e.g., see 4-5 in panel A) are shown.

purified with Ni agarose resin (Qiagen) followed by gel filtration (Sephadex 200 10/300; GE) high-performance liquid chromatography (HPLC), as previously described (9, 24). Binding to SEB, SEC3, and SpeA was examined by enzyme-linked immunosorbent assay (ELISA) and surface plasmon resonance (SPR). In the ELISA, the ELISA wells were coated with individual Vβ proteins (5 μg/ml), followed by addition of various concentrations of the biotin-labeled SAg and streptavidin-conjugated horseradish peroxidase (BD Biosciences). Results were determined by colormetric reaction and absorbance at 450 nm (A_{450}). The affinities and kinetic parameters of Vβ-SAg interactions were determined by SPR analysis using a BIAcore 3000 instrument, as described previously (9, 24).

Computer modeling. Energy minimization of the mutant Vβ8.2(G53K)-SpeA and mVβ8.2(G53R)-SEB complexes was performed using Swiss Protein Data Bank (PDB) DeepView based on the crystal structures of mouse TCR8.2-SpeA and mouse TCR8.2-SEB, respectively (30, 48), using 50 steps of steepest descent and 50 steps on the conjugate gradient. PyMol was used to generate the superimposed structures (RCSB PDB accession codes 1L0X, 1SBB, 1JCK).

T-cell assays. T-cell hybridoma line m6-16 cells displaying mouse Vβ8.2 and CD8 (2×10^6 cells/ml) (20) were stimulated with 25 nM SpeA, in the presence of cells of the MHC class II-positive B-cell line LG-2 (4×10^5 cells/ml). Soluble Vβ proteins (4-5, S5-2, or KKR) were added at various concentrations. After incubation at 37°C for 22 h, cells were centrifuged and supernatants were collected. IL-2 levels were measured by ELISA.

Animal studies. Dutch belted rabbits (1.5 to 2 kg) were used in accordance with guidelines established by the University of Minnesota IACUC. In two sets of experiments, two groups of rabbits ($n = 6$) were administered 5 μg/kg SpeA purified from *Streptococcus* strain 594, followed by injection of 0.15 μg/kg lipopolysaccharide (LPS) from *Salmonella enterica* serovar Typhimurium after 4 h (40). In the control group, SpeA was administered with phosphate-buffered saline (PBS), while in the sample groups 50 μg/kg G5-8 or 100 μg/kg KKR Vβ proteins was added to SpeA for 30 min prior to injection. Pyrogenicity was determined by monitoring body temperatures at 0 h and after 4 h (the maximal response time for SAgs) (40). Survival of rabbits after LPS treatment was monitored over 48 h.

RESULTS

Engineering high-affinity Vβ8 regions against SpeA. We showed previously that it was possible to generate high-affinity (picomolar K_D values) Vβ regions against exotoxins from *S. aureus* and to use soluble forms of the Vβ fragments to neutralize the toxins in animal models (9). In order to generate a potential neutralizing agent against the streptococcal SAg SpeA (53), one of two major SAgs from this organism (SpeC being the other) (34), the Vβ8 region that binds to SpeA with relatively low affinity (K_D = 6.2 μM) (48) was expressed as an Aga2 fusion in a yeast display system (Fig. 1A). As expected due to this low affinity, yeast cells that displayed the wild-type Vβ8 protein did not bind to SpeA at 200 nM, even though the full-length Vβ was expressed at high surface levels, as judged by staining with antibodies to the N-terminal hemagglutinin tag (HA) and the C-terminal c-myc tag (Fig. 1B).

To identify high-affinity Vβ mutants, a library of mutants in CDR2 residues 53 through 57 was screened by cell sorting after incubation with biotin-labeled SpeA (see Fig. 1C for a schematic of the selection process). After four successive sorts with SpeA at 1.5 μM, 200 nM, 50 nM, and 20 nM, respectively, a population of yeast that stained positive with SpeA was identified (data not shown). Yeast clones were examined for SpeA binding by flow cytometry, and several clones including clone 4-5 were found to be positive (Fig. 2A) (data not shown). Plasmids from 30 clones were sequenced, and four unique mutants were identified (Fig. 2B). The first four residues within

the mutated region showed conserved motifs: Arg/Lys at position 53, His at position 54, Val at position 55, and Leu/Met at position 56. Single-site mutations, such as H47Y, outside the mutated region of the libraries were also observed in some clones.

Because we have shown previously that it is possible to generate even higher-affinity mutants by sequential mutagenesis and selection, we also generated libraries (Fig. 1C) in other regions that are known to contact SpeA, using the mutant with the best binding (4-5) from the first generation as a template. The three libraries contained degeneracy in residues 66 to 68 and 70 and 71 of framework 3 and hypervariable 4 regions (FR3/HV4), residues 48 to 50 and 52 of CDR2 (called library CDR2-a), and residues 28 to 30 of CDR1. In order to select for higher-affinity clones, equilibrium-based selections were performed with SpeA at concentrations of 20 nM, 100 pM, and 50 pM (twice) through four rounds of sorting. Twenty to 30 clones from each of these libraries were isolated; analyses of individual clones at various concentrations of SpeA showed that they exhibited improved binding compared to clone 4-5 (see Fig. 2C for CDR2-a clones and Fig. 2D for FR3/HV4 clones) (data not shown).

Sequences of various mutants were determined (Fig. 2B). The CDR2-a library showed preferential mutations at positions 48, 50, and 52, but not a strictly conserved residue at any position. Likewise, clones from the FR3/HV4 library also showed conserved mutations. Mutants from the CDR1 library showed a conserved His at position 28.

Based on flow cytometry analysis, clones S5-2, S5-6, 4e-1, and 4e-10 each exhibited enhanced binding to SpeA (Fig. 2C and D). Clones 4e-1 and 4e-10 had mutation in either CDR1 (N30K) or the HV4 loop (Q74R), respectively, which we predict contributed to the improved binding to SpeA (Fig. 2B). The H41Q mutation in 4e-1 resides outside the Vβ-SpeA interface, suggesting it had less of an effect on SpeA binding. Clones S5-2 and S5-6 had identical mutations in CDR2, except that S5-2 contained an additional mutation at residue 48 (Y48K). Interestingly, although S5-2 and S5-6 differed in only one residue (48), soluble S5-6 had a tendency to aggregate, as revealed by SDS-PAGE, while S5-2 behaved as a monomer (data not shown). While we do not understand the mechanism, the result with the Lys48 mutation has also been observed in another Vβ mutant (data not shown). Since S5-2 and S5-6 shared similar affinities for SpeA, based on flow cytometry analysis, S5-2 was selected for further study.

We have shown previously with Vβ mutants against SEC3 that it is possible to combine the mutations to achieve improvements in affinity (24). Thus, we also generated a combinatorial mutant, called KKR, that contained selected mutations from S5-2, 4e-1, and 4e-10, in addition to the Gly-to-Lys mutation at position 53 (Fig. 2B). Protein KKR with the G53K mutation was pursued further, as the G53R mutation in the context of the other KKR mutations did not yield as high an affinity (data not shown).

Binding of soluble Vβ mutants to SpeA. In order to examine the binding of soluble forms of selected Vβ mutants, mutants 4-5, S5-2, and KKR were expressed in *E. coli*, and the refolded recombinant proteins were purified from inclusion bodies. All three mutants were shown to bind to SpeA in an ELISA (Table 1; see Fig. S1A in the supplemental material). Binding affinities

TABLE 1. Binding properties of high-affinity Vβ8.2 variants to SpeA, SEB, and SEC3 as determined by ELISA and SPR[a]

Vβ8.2 WT or variant	SpeA				SEB				SEC3			
	K_{on} (M^{-1} s^{-1})	K_{off} (s^{-1})	K_D (nM)	BD_{50} (nM)	K_{on} (M^{-1} s^{-1})	K_{off} (s^{-1})	K_D (nM)	BD_{50} (nM)	K_{on} (M^{-1} s^{-1})	K_{off} (s^{-1})	K_D (nM)	BD_{50} (nM)
WT	ND[b]	ND	6.2×10^{3}[c]	ND	ND	ND	1.4×10^{5}[c]	ND	ND	ND	3.0×10^{3}[c]	ND
Variants												
4-5	1.87×10^{5}	9.61×10^{-4}	5	4.4 ± 0.9	2.98×10^{5}	1.97×10^{-2}	66	28 ± 3		No binding		961 ± 30
S5-2	1.94×10^{5}	5.72×10^{-4}	3	5.2 ± 0.7	3.30×10^{5}	1.43×10^{-2}	43	26 ± 3		No binding		1,875 ± 331
KKR	1.85×10^{5}	6.70×10^{-5}	0.27	3.2 ± 0.7	2.20×10^{5}	1.50×10^{-2}	68	16.6 ± 6		No binding		1,511 ± 500
L2CM	4.72×10^{3}	5.82×10^{-4}	123	39 ± 12	ND	ND	491	27 ± 4	3.96×10^{5}	3.94×10^{-3}	10	1.3 ± 0.9
G5-8	4.82×10^{5}	2.17×10^{-3}	5	4.5 ± 0.9	5.75×10^{5}	1.40×10^{-4}	0.24	1.5 ± 1		No binding		488 ± 87
G5-8(R53G)	ND	ND	525	12 ± 7	5.05×10^{5}	3.57×10^{-3}	7	3.9 ± 0.3	3.22×10^{5}	1.11×10^{-2}	35	4.4 ± 1.9

[a] Throughout, the BD_{50} (50% binding dose) was the concentration of soluble Vβs that yielded 50% maximal binding for SAgs as determined by ELISA and was used as an indication of binding properties of Vβs against SAgs. All other binding values were obtained by SPR.
[b] ND, not determined.
[c] Previously reported values from WT Vβ8 K_D with SAgs (11, 31, 48).

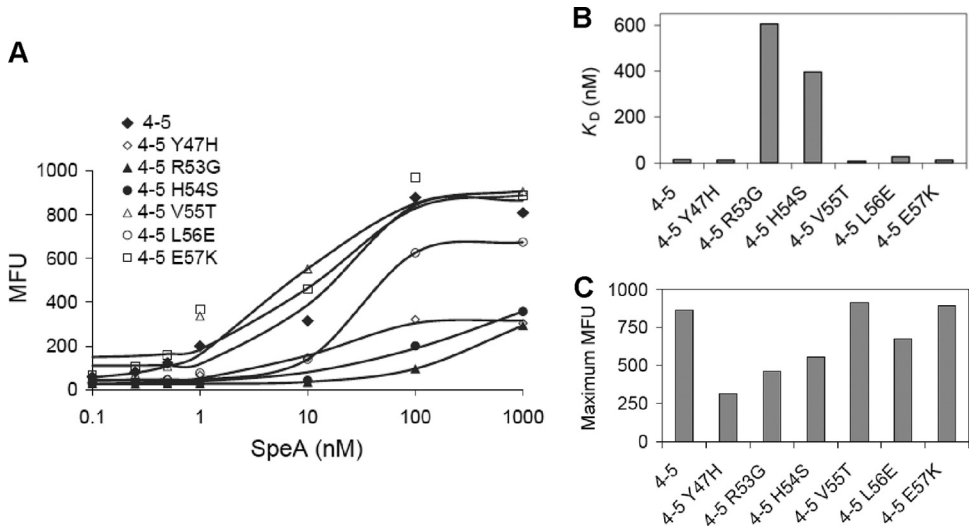

FIG. 3. Analysis of single-site reverse mutants of SpeA high-affinity Vβ clone 4-5. (A) Six 4-5 clones, each with a single-site reversion mutation (to wild-type residue) and mutant 4-5 were transformed into yeast and titrated with biotin-labeled SpeA. (B) The concentration of SpeA that yielded 50% maximal binding is shown as an estimate of K_D. (C) Maximal fluorescence, as indicated by the mean fluorescence units (MFU) at saturation, for each mutant was determined by flow cytometry.

and kinetics of the mutants were determined by SPR with immobilized SpeA (Table 1; see Fig. S2A in the supplemental material) (data not shown). SPR analysis showed that all three high-affinity mutants had similar on-rates (K_{on}), but the third generation, combinatorial mutant KKR had a 20-fold slower off-rate (K_{off}) and improved affinity (K_D, ~270 pM) (Table 1).

Basis of high-affinity SpeA binding by the Vβ8 mutants. Based on our SPR analyses, one or more of the six mutations in mutant 4-5 accounted for at least a 1,000-fold increase in affinity compared to that in WT Vβ8. To further explore the molecular basis of the high-affinity binding, we generated the six reversion mutants of the 4-5 protein and examined them in the yeast display system. This approach allows more rapid analysis than expression of soluble mutants, because titrations of yeast-displayed mutants can be performed without the need for protein purification (10). Flow cytometry-based titrations of each mutant with SpeA (Fig. 3A) were used to calculate the concentration of SpeA that yielded 50% maximal binding, an estimate of the relative K_D values of the protein (Fig. 3B). The maximum fluorescence (mean fluorescence units [MFU]) at saturation for each mutant varied to some extent (Fig. 3A and C) and is a property of the stability of the Vβ protein (44). Thus, the Y47H mutation was expressed at about 30% of the surface level of the 4-5 protein, consistent with this mutation providing enhanced stability to the Vβ8 protein (9). Similarly, the Leu56Glu mutation appeared to influence primarily the maximum MFU. Only two revertants, Arg53Gly and His54Ser, showed substantial reductions in binding (Fig. 3B). Estimates of the magnitude of the effect on binding indicate that the Arg53 mutation has at least a 100-fold impact on affinity.

Cross-reactivity of soluble Vβ mutants for SpeA, SEB, and SEC3. During the course of this work, we observed that high-affinity Vβ8 mutant G5-8, generated against SEB, also contained Gly53Arg and Thr55Val mutations (Fig. 2B) (9), two of the highly restricted substitutions found in the 4-5 and S5-2 generation of mutants. In addition, yeast-displayed G5-8 was shown to stain positively with SpeA (data not shown). Thus, this mutant and a Vβ mutant called L2CM that lacked these mutations (Fig. 2B) (24) but contained mutations that yielded high affinity for binding to SEC3 were also expressed and purified from *E. coli*. Interestingly, G5-8 exhibited high-affinity binding to SpeA, whereas L2CM had intermediate affinity, albeit above the affinity of WT Vβ8.2 (Table 1; see Fig. S1A and S2A in the supplemental material). The lower affinity of L2CM was in part due to a 30-fold-slower on-rate for SpeA compared to KKR and 100-fold slower on-rate compared to G5-8.

Given the unexpected cross-reactivity of the high-affinity mutant G5-8 for SpeA, we proceeded to examine whether each of the high-affinity proteins generated against SpeA, SEB, or SEC3 cross-reacted with high affinity against the other members of this SAg subfamily. To measure the extent of cross-reactivity, we performed both ELISAs and SPR experiments. In the ELISA format, the five high-affinity Vβ proteins were immobilized on wells and assayed with serial dilutions of biotin-labeled SAg. The concentration of soluble Vβ that yielded 50% maximal binding (50% binding dose [BD_{50}]) was determined (Table 1) for each of the five proteins (4-5, S5-2, KKR, G5-8, and L2CM) and the three SAgs (SpeA, SEB, and SEC3). In the case of each SAg, the Vβ protein originally engineered for high affinity yielded the highest affinity (i.e., lowest BD_{50} value), as expected. As indicated above, G5-8 cross-reacted with SpeA in this assay almost as well as the three proteins generated against SpeA, 4-5, S5-2, and KKR. Each of the latter proteins also cross-reacted with SEB, albeit at about 10-fold lower affinity than G5-8. In contrast, L2CM, which was generated against SEC3, cross-reacted less well with SpeA. As previously noted, L2CM had higher affinity for SEB than the WT Vβ8 protein (24), but its affinity was well below that of G5-8 (9). The extents of cross-reactivities among the Vβ proteins and the three SAgs were also measured by SPR (Table 1; see Fig. S2 in the supplemental material). These results verified

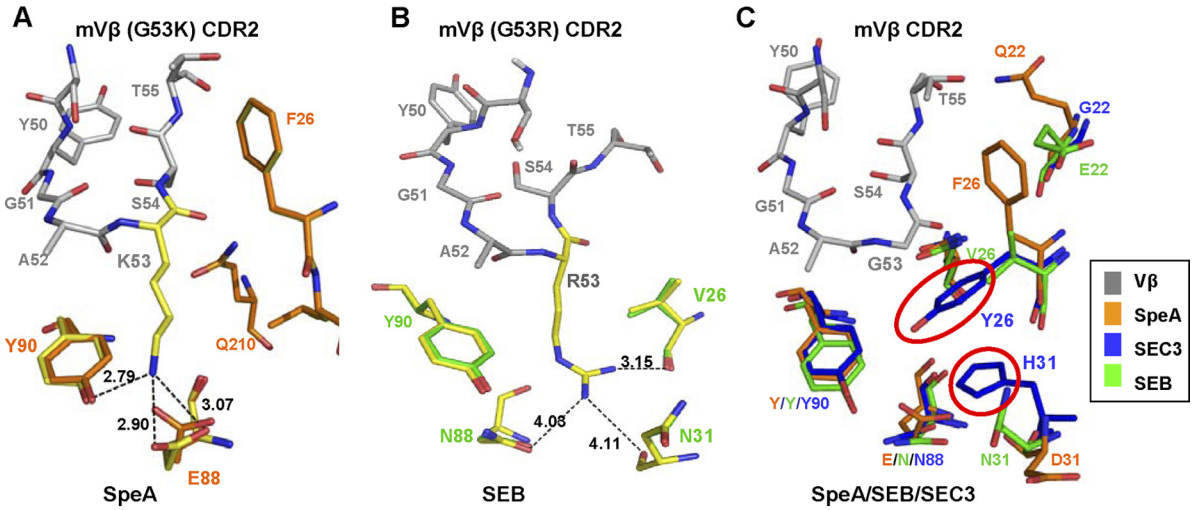

FIG. 4. Structures and models of mVβ8.2 interactions with SpeA, SEC3, and SEB. (A) Energy-minimized computer model of the mVβ8.2(G53K)-SpeA complex; (B) energy-minimized computer model of the mVβ8.2(G53R)-SEB complex. (C) Residues of SpeA (orange), SEC3 (blue), and SEB (green) that are at the interface were superimposed in complexes with mouse Vβ8.2 CDR2 loop (gray). (RCSB PDB accession code 1L0X, 1SBB, 1JCK).

that the high-affinity Vβ regions generated against SpeA cross-reacted with SEB to a much greater extent but could scarcely bind SEC3. Similarly, the high-affinity Vβ proteins generated against SEB cross-reacted with SpeA to a greater extent than they did with SEC3, which was undetectable by SPR.

Possible structural basis of cross-reactivities. The cross-reactivities of high-affinity Vβs would not be predicted from primary sequence similarities among the three toxins, since SEB and SEC3 share the highest sequence homology (65%) among the three SAgs. To explore the molecular basis, we examined the sequences of the high-affinity Vβ mutants, as well as the three SAgs (Fig. 2B; see Fig. S3 in the supplemental material). In the high-affinity Vβ, the G53R/K mutation of CDR2, shown to be most important for high affinity against SpeA, was the one of two conserved mutations (T55V being the other) shared among the high-affinity mutants generated against SEB and SpeA, but it was not selected in mutants against SEC3, including L2CM (24; data not shown). Energy-minimized computer models of the Lys53 and Arg53 single-site mutants in complex with SpeA and SEB, respectively, (Fig. 4A and B) support the notion that the side chains of these mutations could stabilize the interaction with SpeA/SEB residues: e.g., through the backbone carbonyl oxygen of SEB(Val26), SEB(Asn31), and side-chain oxygen of SEB(Asn88), SpeA (Tyr90), and SpeA(Glu88).

The question of why these mutations would have a detrimental effect on binding to SEC3 remained. To explore this further, we focused our attention on the region of the SAgs in contact with CDR2, from residues 19 to 26 (Fig. 4C; see Fig. S3 in the supplemental material). In this region, there was only one position where SEB and SpeA were more similar than SEC3: residue 22 (Gln in SpeA, Glu in SEB, and Gly in SEC3). However, the structure of this region showed that the side chains of Gln in SpeA and the side chain of Glu in SEB are pointed in different directions (Fig. 4C). Furthermore, these side chains are not near residue 53 in Vβ8, the mutation shown to be most important in binding of SpeA (e.g., Gly53 of Vβ8 and Glu22 of SEB are 9 Å apart). In contrast, residue 26 of the SAgs directly opposes residue 53 of Vβ8 (Fig. 4C). Interestingly, although the residues at position 26 are more conserved between SpeA (Phe) and SEC3 (Tyr) than SEB (Val), the structures of the three SAgs show that the phenyl ring of Tyr26 in SEC3 is pointed in a different direction from the ring from Phe26 of SpeA or the side chain from Val26 of SEB (perhaps due to stacking interactions of Tyr26 with His31 in SEC3). Thus, the side chain of the arginine at residue 53 in the high-affinity Vβ mutants could be accommodated in the pocket formed in SpeA and SEB, in a position that may pose a steric hindrance due to the side chain of Tyr26 in SEC3. Alternatively, H31 itself may contribute to steric hindrance of the G53K/R mutations in KKR and G5-8. Regardless, Y26, H31, or both appear to disallow accommodation of the CDR2 mutation at position 53.

To verify the role of the Arg53 mutation, we generated soluble protein of the revertant (R53G) in G5-8 and performed the quantitative ELISA and SPR (Table 1). As with the 4-5 R53G revertant binding to SpeA, the G5-8 revertant exhibited reduced binding to its selecting ligand, SEB. More interestingly, the R53G mutant of G5-8 now exhibited considerably higher-affinity binding to SEC3 (K_D = 35 nM), supporting the premise that the side chain of Arg53 leads to a steric clash with SEC3.

Ability of soluble Vβ proteins to inhibit the biological activity of SpeA. To determine whether the soluble forms of the high-affinity Vβ proteins engineered against the streptococcal toxin SpeA were capable of inhibiting the *in vitro* activity of the T cells stimulated with SpeA, an assay was conducted in which a Vβ8-positive T-cell line was stimulated with SpeA (25 nM), in the presence of an MHC class II-positive antigen-presenting cell line. The amount of IL-2 released upon stimulation was assayed by ELISA. At the highest concentration of antagonist, each of the four high-affinity Vβ proteins (4-5, S5-2, KKR, and G5-8) was able to inhibit completely the IL-2 release mediated by SpeA (Fig. 5A). The 50% inhibitory concentrations (IC_{50}s)

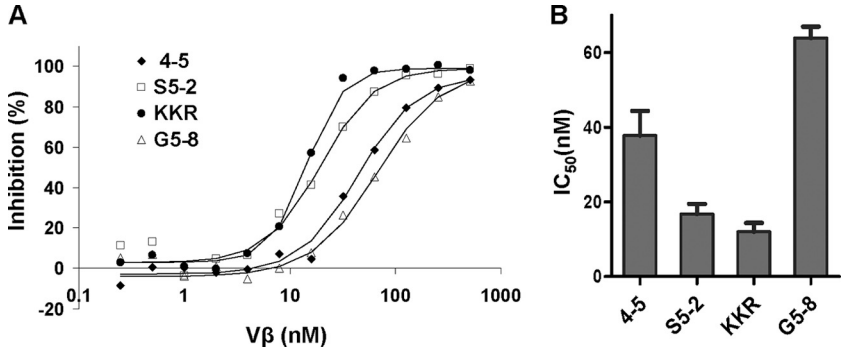

FIG. 5. Neutralization of SpeA-mediated T-cell activation with soluble high-affinity Vβ mutants. (A) T-cell hybridoma ($V\beta8^+$), antigen-presenting cells, 25 nM SpeA, and 1:2 serial dilutions of soluble high-affinity Vβ mutants were incubated at 37°C overnight, and IL-2 released in supernatants was assayed by ELISA. The percent inhibition of T-cell activity in the presence of different concentrations of Vβ was calculated as $(A_{450}$ *no inhibitor* $- A_{450}$ *inhibitor*$)/A_{450}$ *no inhibitor* $\times$ 100. (B) Half-maximal inhibitory concentration (IC_{50}) of IL-2 secretion by the Vβ mutants. Data are expressed as the mean of two independent experiments of duplicate samples.

of the inhibitors correlated well with the binding affinity of the Vβ measured by SPR (Fig. 5B and Table 1). Accordingly, the KKR mutant showed the most effective inhibition, providing a possible candidate for subsequent studies to neutralize the toxic activity of SpeA in animal models.

Soluble Vβ mutants neutralize SpeA in animal models. To examine whether the high-affinity Vβ variants can neutralize SpeA activity *in vivo*, we tested the two soluble Vβ proteins (G5-8 and KKR) with high affinity for SpeA in an endotoxin-enhanced rabbit lethality model. Previously, we showed that this model functions as a model of TSS in which the time of lethality is significantly shortened compared to those in other rabbit models, but like other models depends on production of high levels of TNF-α and IL-1β (17). Two groups of rabbits (n = 6/group) were administered 5 μg/kg SpeA purified from *Streptococcus* strain 594, with subsequent injection of 0.15 μg/kg lipopolysaccharide (LPS; 1/2,500 lethal dose, 50% endpoint) from *S.* Typhimurium after 4 h. In the control group, SpeA was administered in PBS alone, while in the other group, 50 to ~100 μg/kg Vβ was premixed with SpeA at 37°C for 30 min before injection. Pyrogenicity was assessed by monitoring temperatures at time zero and after 4 h (the maximal response period of time for SAgs and just before LPS administration). Survival of the rabbits after LPS treatment was monitored at 48 h (Fig. 6).

In two independent experiments, the rabbits in the control groups treated with SpeA alone developed fever with an elevation of body temperature of ~1.4 to 1.6°C after 4 h (Fig. 6A and C). The six rabbits injected with SpeA and the KKR Vβ exhibited a mild but not significant increase in body temperature of ~0.4°C after 4 h (Fig. 6A), and 5 of 6 rabbits survived, compared to 0 of 6 in the control group (Fig. 6B). The six rabbits injected with SpeA and the G5-8 Vβ did not show elevation of body temperature (Fig. 6C), and all six of the rabbits survived after administration of LPS (Fig. 6D). Thus, both of the high-affinity Vβ mutants were able to protect rabbits from SpeA-mediated pyrogenicity and LPS-induced lethality. The same experiment was performed with rabbits treated with SEC3 alone and with G5-8, and the high-affinity Vβ mutant did not provide significant protection, compared to treatment with SEC3 alone, from either fever or enhanced LPS-induced lethality (data not shown).

DISCUSSION

Invasive diseases, such as TSS, caused by *Streptococcus pyogenes* (group A streptococci [GAS]) have seen increases worldwide (12, 16, 27, 34, 45). Due to its virulence, 30% to 70% of patients suffering streptococcal TSS have died despite treatments, which are largely limited to supportive care, antibiotics, and possibly activated protein C and intravenous immunoglob-

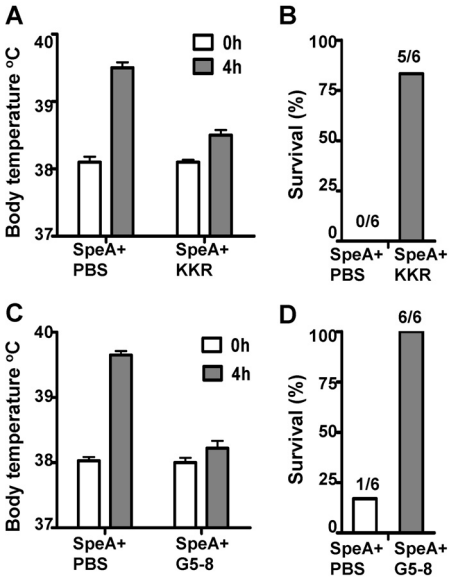

FIG. 6. Soluble Vβ mutants protect rabbits from SpeA-mediated pyrogenicity and endotoxin-induced lethality. (A and B) SpeA (5 μg/kg) in PBS (SpeA only) or with Vβ KKR (100 μg/kg KKR) or (C and D) G5-8 (50 μg/kg) was administered to two groups of rabbits (n = 6), followed by intravenous injection of LPS (0.15 μg/kg) after 4 h. (A and C) Pyrogenicity was assessed by monitoring body temperatures at 0 h (open bars) and 4 h (solid bars). (B and D) Survival of rabbits administered SpeA alone (open bars) or in combination with KKR (B) or G5-8 (D) (solid bars) was monitored over a 48-h period.

ulin (13, 23, 27). The actions of different SAgs from *Streptococcus pyogenes* (36) almost certainly vary, depending on many factors, such as the bacteria and the host, including the MHC (22, 26, 37). Administration of a high dose of intravenous (i.v.) immunoglobin (0.5 to ~1 g/kg) has shown some effectiveness in lowering mortality rates, but its success is limited due to variability in preparations as a consequence of differences in donors, including their history of microbial exposure (27). New therapies are required to neutralize the SAg-mediated effects in TSS caused by *S. aureus* and *Streptococcus pyogenes.*

As SpeA is considered one of the major virulence factors in streptococcal TSS (12, 14, 46), various approaches have been explored to neutralize its toxic activity. These include efforts to develop SpeA toxoid vaccines that induce neutralizing antibodies (5, 33, 38, 51, 52) or the generation of monoclonal antibodies, potentially for passive therapy (49). Our approach has involved the use of soluble, high-affinity receptors that could neutralize the toxins in much the same way as the TNF-α-neutralizing agent Enbrel, a soluble form of the TNF-α receptor, neutralizes its target (6). Our previous success in animal models using a soluble high-affinity Vβ domain against SEB (G5-8) suggested that this approach has potential (9, 21). Here, we have generated high-affinity Vβ against SpeA and explored the possible uses of Vβ agents in neutralizing multiple SAgs, such that the same drug might be used against different infectious agents. The success of this approach depends, among other things, on the structural relatedness of the SAgs and the ability of the neutralizing agents to cross-react with multiple SAgs.

We describe here, for the first time, that it is possible to generate a Vβ mutant, KKR, with picomolar affinity for SpeA and to use a soluble form of this mutant as a potent *in vitro* and *in vivo* neutralizing agent. The high affinity of the Vβ mutants was shown to be due to two mutations in the CDR2 (at positions 53 and 54) but also likely involved the conserved mutations selected in CDR1 (Lys30) and HV4 (Arg72). The composite mutant KKR Vβ thus provides a possible therapeutic agent for diseases that are mediated by this common GAS SAg. As shown recently with G5-8 and the inhibition of lethality and skin reactivity caused by SEB (9, 21), it is thus now possible to directly test the role of SpeA in disease by using soluble forms of KKR.

Unexpectedly, we also found that KKR could bind with high affinity to SEB and that G5-8 could bind with high affinity to SpeA. From a clinical perspective, this could be valuable in that the same neutralizing agent might be useful (e.g., from a regulatory and manufacturing perspective) for diseases caused by two different infectious agents. This pattern of cross-reactivity and the lack of high-affinity binding of these Vβ mutants to SEC3 were surprising based on the sequence similarities of these SAgs. We further showed that the basis of this cross-reactivity, or lack thereof, appears to be controlled by one or two residues, at positions 26 and/or 31, which differ among all three toxins. The higher-affinity cross-reactivity of the SEC3-reactive Vβ mutant L2CM with SSA, but not SEG, has also been described (18). This suggests that Vβ L2CM might also be further optimized by engineering, guided by rational design, in order to neutralize multiple toxins.

These subtle yet significant structural differences among the exotoxins highlight the importance of understanding the details in the design of either toxoid vaccines, or protein-based drugs, against the toxins. For example, in a toxoid-based approach, it would be valuable to elicit antibodies against this epitope since it is directly involved in contact with the cellular receptor. It is likely that such antibodies will also vary in their cross-reactivity, depending on the same differences among SAgs. In fact, this finding may explain the results of an early study (5) that showed some ability of SpeA to induce antibodies with neutralizing potential against SEB, even though there was much less cross-reactivity by ELISA (e.g., a minor fraction of antibodies against the important SAg epitope from residues 19 to 26 could be responsible for neutralization). Hence, a cross-reactive SEB, SEC3, and SpeA toxoid might involve the mutations of residue 26 to optimize antibody cross-reactions with all three SAgs.

The observation that the Vβ variant G5-8 was able to neutralize SpeA and SEB (9) shows that it is possible to use a structure-based strategy to generate high-affinity neutralizing agents that can cross-react with multiple exotoxins. One of the potential advantages of the soluble Vβ approach, compared to antibodies, for example, is that the high-affinity interactions involve precisely the epitope on the SAg that is required for binding of the cellular receptor. In principle, this provides a restriction on the variants of the SAg that might avoid neutralization since such variation might also lead to inability to bind the cellular receptor required for toxicity. In addition, antibodies against SAgs could also mediate undesirable Fc-dependent interactions that facilitate SAg presentation to T cells and cellular activation.

ACKNOWLEDGMENTS

We thank the staff of University of Illinois Biotechnology Center for assistance with flow sorting and DNA sequencing.

This work was supported by NIH grants AI064611 (to D.M.K. and P.M.S.) and AI065690 (to E.J.S.), as well as a grant (U54 AI57153) from the NIH-supported Great Lakes Regional Center for Excellence (to P.M.S. and D.M.K.).

REFERENCES

1. **Abe, J., B. L. Kotzin, K. Jujo, M. E. Melish, M. P. Glode, T. Kohsaka, and D. Y. Leung.** 1992. Selective expansion of T cells expressing T-cell receptor variable regions V beta 2 and V beta 8 in Kawasaki disease. Proc. Natl. Acad. Sci. U. S. A. **89:**4066–4070.
2. **Andersen, P. S., C. Geisler, S. Buus, R. A. Mariuzza, and K. Karjalainen.** 2001. Role of TCR-ligand affinity in T cell activation by bacterial superantigens. J. Biol. Chem. **276:**33452–33457.
3. **Bachert, C., P. Gevaert, N. Zhang, T. van Zele, and C. Perez-Novo.** 2007. Role of staphylococcal superantigens in airway disease. Chem. Immunol. Allergy **93:**214–236.
4. **Bergdoll, M. S., and P. M. Schlievert.** 1984. Toxic-shock syndrome toxin. Lancet **ii:**691.
5. **Bohach, G. A., C. J. Hovde, J. P. Handley, and P. M. Schlievert.** 1988. Cross-neutralization of staphylococcal and streptococcal pyrogenic toxins by monoclonal and polyclonal antibodies. Infect. Immun. **56:**400–404.
6. **Brower, V.** 1997. Enbrel's phase III reinforces prospects in RA. Nat. Biotechnol. **15:**1240.
7. **Bubeck Wardenburg, J., R. J. Patel, and O. Schneewind.** 2007. Surface proteins and exotoxins are required for the pathogenesis of *Staphylococcus aureus* pneumonia. Infect. Immun. **75:**1040–1044.
8. **Bueno, C., C. D. Lemke, G. Criado, M. L. Baroja, S. S. Ferguson, A. K. Rahman, C. D. Tsoukas, J. K. McCormick, and J. Madrenas.** 2006. Bacterial superantigens bypass Lck-dependent T cell receptor signaling by activating a Galpha11-dependent, PLC-beta-mediated pathway. Immunity **25:**67–78.
9. **Buonpane, R. A., H. R. Churchill, B. Moza, E. J. Sundberg, M. L. Peterson, P. M. Schlievert, and D. M. Kranz.** 2007. Neutralization of staphylococcal enterotoxin B by soluble, high-affinity receptor antagonists. Nat. Med. **13:**725–729.
10. **Buonpane, R. A., B. Moza, E. J. Sundberg, and D. M. Kranz.** 2005. Characterization of T cell receptors engineered for high affinity against toxic shock syndrome toxin-1. J. Mol. Biol. **353:**308–321.

11. **Churchill, H. R., P. S. Andersen, E. A. Parke, R. A. Mariuzza, and D. M. Kranz.** 2000. Mapping the energy of superantigen Staphylococcus enterotoxin C3 recognition of an alpha/beta T cell receptor using alanine scanning mutagenesis. J. Exp. Med. **191:**835–846.
12. **Cleary, P. P., E. L. Kaplan, J. P. Handley, A. Wlazlo, M. H. Kim, A. R. Hauser, and P. M. Schlievert.** 1992. Clonal basis for resurgence of serious Streptococcus pyogenes disease in the 1980s. Lancet **339:**518–521.
13. **Cone, L. A., R. A. Stone, P. M. Schlievert, R. A. Sneider, A. M. Rubin, K. Jesser, and S. W. Renker.** 2006. An early favorable outcome of streptococcal toxic shock syndrome may require a combination of antimicrobial and intravenous gamma globulin therapy together with activated protein C. Scand. J. Infect. Dis. **38:**960–963.
14. **Cone, L. A., D. R. Woodard, P. M. Schlievert, and G. S. Tomory.** 1987. Clinical and bacteriologic observations of a toxic shock-like syndrome due to Streptococcus pyogenes. N. Engl. J. Med. **317:**146–149.
15. **Davis, J. P., P. J. Chesney, P. J. Wand, and M. LaVenture.** 1980. Toxic-shock syndrome: epidemiologic features, recurrence, risk factors, and prevention. N. Engl. J. Med. **303:**1429–1435.
16. **Demers, B., A. E. Simor, H. Vellend, P. M. Schlievert, S. Byrne, F. Jamieson, S. Walmsley, and D. E. Low.** 1993. Severe invasive group A streptococcal infections in Ontario, Canada: 1987–1991. Clin. Infect. Dis. **16:**792–802.
17. **Dinges, M. M., and P. M. Schlievert.** 2001. Comparative analysis of lipopolysaccharide-induced tumor necrosis factor alpha activity in serum and lethality in mice and rabbits pretreated with the staphylococcal superantigen toxic shock syndrome toxin 1. Infect. Immun. **69:**7169–7172.
18. **Fernandez, M. M., S. Bhattacharya, M. C. De Marzi, P. H. Brown, M. Kerzic, P. Schuck, R. A. Mariuzza, and E. L. Malchiodi.** 2007. Superantigen natural affinity maturation revealed by the crystal structure of staphylococcal enterotoxin G and its binding to T-cell receptor Vbeta8.2. Proteins **68:**389–402.
19. **Fields, B. A., E. L. Malchiodi, H. Li, X. Ysern, C. V. Stauffacher, P. M. Schlievert, K. Karjalainen, and R. A. Mariuzza.** 1996. Crystal structure of a T-cell receptor b-chain complexed with a superantigen. Nature **384:**188–192.
20. **Holler, P. D., and D. M. Kranz.** 2003. Quantitative analysis of the contribution of TCR/pepMHC affinity and CD8 to T cell activation. Immunity **18:**255–264.
21. **John, C. C., M. Niermann, B. Sharon, M. L. Peterson, D. M. Kranz, and P. M. Schlievert.** 2009. Staphylococcal toxic shock syndrome erythroderma is associated with superantigenicity and hypersensitivity. Clin. Infect. Dis. **49:**1893–1896.
22. **Kansal, R. G., V. Datta, R. K. Aziz, N. F. Abdeltawab, S. Rowe, and M. Kotb.** 2010. Dissection of the molecular basis for hypervirulence of an in vivo-selected phenotype of the widely disseminated M1T1 strain of group A Streptococcus bacteria. J. Infect. Dis. **201:**855–865.
23. **Kaul, R., A. McGeer, A. Norrby-Teglund, M. Kotb, B. Schwartz, K. O'Rourke, J. Talbot, and D. E. Low.** 1999. Intravenous immunoglobulin therapy for streptococcal toxic shock syndrome—a comparative observational study. The Canadian Streptococcal Study Group. Clin. Infect. Dis. **28:**800–807.
24. **Kieke, M. C., E. Sundberg, E. V. Shusta, R. A. Mariuzza, K. D. Wittrup, and D. M. Kranz.** 2001. High affinity T cell receptors from yeast display libraries block T cell activation by superantigens. J. Mol. Biol. **307:**1305–1315.
25. **Kline, J. B., and C. M. Collins.** 1996. Analysis of the superantigenic activity of mutant and allelic forms of streptococcal pyrogenic exotoxin A. Infect. Immun. **64:**861–869.
26. **Kotb, M., A. Norrby-Teglund, A. McGeer, H. El-Sherbini, M. T. Dorak, A. Khurshid, K. Green, J. Peeples, J. Wade, G. Thomson, B. Schwartz, and D. E. Low.** 2002. An immunogenetic and molecular basis for differences in outcomes of invasive group A streptococcal infections. Nat. Med. **8:**1398–1404.
27. **Lappin, E., and A. J. Ferguson.** 2009. Gram-positive toxic shock syndromes. Lancet Infect. Dis. **9:**281–290.
28. **Leung, D. Y., R. C. Giorno, L. V. Kazemi, P. A. Flynn, and J. B. Busse.** 1995. Evidence for superantigen involvement in cardiovascular injury due to Kawasaki syndrome. J. Immunol. **155:**5018–5021.
29. **Li, H., A. Llera, E. L. Malchiodi, and R. A. Mariuzza.** 1999. The structural basis of T cell activation by superantigens. Annu. Rev. Immunol. **17:**435–466.
30. **Li, H., A. Llera, D. Tsuchiya, L. Leder, X. Ysern, P. M. Schlievert, K. Karjalainen, and R. A. Mariuzza.** 1998. Three-dimensional structure of the complex between a T cell receptor beta chain and the superantigen staphylococcal enterotoxin B. Immunity **9:**807–816.
31. **Malchiodi, E. L., E. Eisenstein, B. A. Fields, D. H. Ohlendorf, P. M. Schlievert, K. Karjalainen, and R. A. Mariuzza.** 1995. Superantigen binding to a T cell receptor b chain of known three-dimensional structure. J. Exp. Med. **182:**1833–1845.
32. **Marrack, P., and J. Kappler.** 1990. The staphylococcal enterotoxins and their relatives. Science **248:**705–711.
33. **McCormick, J. K., T. J. Tripp, S. B. Olmsted, Y. V. Matsuka, P. J. Gahr, D. H. Ohlendorf, and P. M. Schlievert.** 2000. Development of streptococcal pyrogenic exotoxin C vaccine toxoids that are protective in the rabbit model of toxic shock syndrome. J. Immunol. **165:**2306–2312.
34. **McCormick, J. K., J. M. Yarwood, and P. M. Schlievert.** 2001. Toxic shock syndrome and bacterial superantigens: an update. Annu. Rev. Microbiol. **55:**77–104.
35. **Pragman, A. A., J. M. Yarwood, T. J. Tripp, and P. M. Schlievert.** 2004. Characterization of virulence factor regulation by SrrAB, a two-component system in *Staphylococcus aureus*. J. Bacteriol. **186:**2430–2438.
36. **Proft, T., S. L. Moffatt, C. J. Berkahn, and J. D. Fraser.** 1999. Identification and characterization of novel superantigens from Streptococcus pyogenes. J. Exp. Med. **189:**89–102.
37. **Proft, T., B. Schrage, and J. D. Fraser.** 2007. The cytokine response to streptococcal superantigens varies between individual toxins and between individuals: implications for the pathogenesis of group A streptococcal diseases. J. Interferon Cytokine Res. **27:**553–557.
38. **Roggiani, M., J. A. Stoehr, S. B. Olmsted, Y. V. Matsuka, S. Pillai, D. H. Ohlendorf, and P. M. Schlievert.** 2000. Toxoids of streptococcal pyrogenic exotoxin A are protective in rabbit models of streptococcal toxic shock syndrome. Infect. Immun. **68:**5011–5017.
39. **Schlievert, P. M.** 2009. Cytolysins, superantigens, and pneumonia due to community-associated methicillin-resistant Staphylococcus aureus. J. Infect. Dis. **200:**676–678.
40. **Schlievert, P. M.** 1982. Enhancement of host susceptibility to lethal endotoxin shock by staphylococcal pyrogenic exotoxin type C. Infect. Immun. **36:**123–128.
41. **Schlievert, P. M., K. N. Shands, B. B. Dan, G. P. Schmid, and R. D. Nishimura.** 1981. Identification and characterization of an exotoxin from Staphylococcus aureus associated with toxic-shock syndrome. J. Infect. Dis. **143:**509–516.
42. **Schlievert, P. M., K. L. Strandberg, Y. C. Lin, M. L. Peterson, and D. Y. Leung.** 2010. Secreted virulence factor comparison between methicillin-resistant and methicillin-sensitive Staphylococcus aureus, and its relevance to atopic dermatitis. J. Allergy Clin. Immunol. **125:**39–49.
43. **Shands, K. N., G. P. Schmid, B. B. Dan, D. Blum, R. J. Guidotti, N. T. Hargrett, R. L. Anderson, D. L. Hill, C. V. Broome, J. D. Band, and D. W. Fraser.** 1980. Toxic-shock syndrome in menstruating women: association with tampon use and Staphylococcus aureus and clinical features in 52 cases. N. Engl. J. Med. **303:**1436–1442.
44. **Shusta, E. V., M. C. Kieke, E. Parke, D. M. Kranz, and K. D. Wittrup.** 1999. Yeast polypeptide fusion surface display levels predict thermal stability and soluble secretion efficiency. J. Mol. Biol. **292:**949–956.
45. **Stevens, D. L.** 1995. Streptococcal toxic-shock syndrome: spectrum of disease, pathogenesis, and new concepts in treatment. Emerg. Infect. Dis. **1:**69–78.
46. **Stevens, D. L., M. H. Tanner, J. Winship, R. Swarts, K. M. Ries, P. M. Schlievert, and E. Kaplan.** 1989. Severe group A streptococcal infections associated with a toxic shock-like syndrome and scarlet fever toxin A. N. Engl. J. Med. **321:**1–7.
47. **Sundberg, E. J.** 2009. Molecular recognition of diverse ligands by T-cell receptors. Methods Mol. Biol. **524:**347–359.
48. **Sundberg, E. J., H. Li, A. S. Llera, J. K. McCormick, J. Tormo, P. M. Schlievert, K. Karjalainen, and R. A. Mariuzza.** 2002. Structures of two streptococcal superantigens bound to TCR beta chains reveal diversity in the architecture of T cell signaling complexes. Structure (Camb.) **10:**687–699.
49. **Tilahun, M. E., G. Rajagopalan, N. Shah-Mahoney, R. G. Lawlor, A. Y. Tilahun, C. Xie, K. Natarajan, D. H. Margulies, D. I. Ratner, B. A. Osborne, and R. A. Goldsby.** 2010. Potent neutralization of staphylococcal enterotoxin B by synergistic action of chimeric antibodies. Infect. Immun. **78:**2801–2811.
50. **Todd, J., M. Fishaut, F. Kapral, and T. Welch.** 1978. Toxic-shock syndrome associated with phage-group-I staphylococci. Lancet **ii:**1116–1118.
51. **Ulrich, R. G.** 2008. Vaccine based on a ubiquitous cysteinyl protease and streptococcal pyrogenic exotoxin A protects against Streptococcus pyogenes sepsis and toxic shock. J. Immune Based Ther. Vaccines **6:**8.
52. **Ulrich, R. G., M. A. Olson, and S. Bavari.** 1998. Development of engineered vaccines effective against structurally related bacterial superantigens. Vaccine **16:**1857–1864.
53. **Weeks, C. R., and J. J. Ferretti.** 1986. Nucleotide sequence of the type A streptococcal exotoxin (erythrogenic toxin) gene from *Streptococcus pyogenes* bacteriophage T12. Infect. Immun. **52:**144–150.